*NASA Contractor Report 4758*

# Application of AWE for RCS frequency response calculations using Method of Moments

C.J.Reddy
*Hampton University, Hampton, Virginia*

M.D.Deshpande
*ViGYAN Inc., Hampton, Virginia*

October 1996

National Aeronautics and
Space Administration
Langley Research Center
Hampton, Virginia 23681-0001

# CONTENTS

# Abstract

An implementation of the Asymptotic Waveform Evaluation (AWE) technique is presented for obtaining the frequency response of the Radar Cross Section (RCS) of arbitrarily shaped three dimensional perfect electric conductor(PEC) bodies. An Electric Field Integral Equation (EFIE) is solved using the Method of Moments (MoM) to compute the RCS. The electric current, thus obtained is expanded in a Taylor series around the frequency of interest. The coefficients of the Taylor series (called “moments”) are obtained using the frequency derivatives of the EFIE. Using the moments, the electric current on the PEC body is obtained over a frequency band. Using the electric current at differenct frequencies, RCS of the PEC body is obtained over a wide frequency band. Numerical results for a square plate, a cube, and a sphere are presented over a bandwidth. A good agreement between AWE and the exact solution over the bandwidth is observed.

# List of Symbols

| | |
|---|---|
| $\alpha$ | Polarization angle of the incident electric field |
| $\nabla$ | Del operator |
| $\delta_{qo}$ | Kronecker delta defined in equation (21) |
| $\eta_o$ | Free space intrinsic impedance $377\Omega$ |
| $\hat{\theta}$ | Unit normal vector along $\theta$ direction |
| $\hat{\phi}$ | Unit normal vector along $\phi$ direction |
| $(\theta_i, \phi_i)$ | Incident angles |
| $\sigma$ | Radar Cross Section |
| $A$ | Area of the triangle |
| AWE | Asymptotic Waveform Evaluation |
| $ds$ | Surface integration with respect to observation coordinates |
| $ds'$ | Surface integration with respect to source coordinates |
| EFIE | Electric Field Integral Equation |
| $\mathbf{E}_{inc}$ | Incident Electric field |
| $\mathbf{E}_i$ | Amplitude of the incident electric field |
| $\mathbf{E}_{fscat}$ | Scattered electric far field |
| $\mathbf{E}_{scat}$ | Scattered Electric field |
| $E_x$ | x component of $\mathbf{E}_i$ |
| $E_y$ | y component of $\mathbf{E}_i$ |

| | |
|---|---|
| $E_z$ | z component of $\mathbf{E}_i$ |
| $f$ | Frequency |
| $I(k)$ | Unknown coefficient vector as a function of $k$ |
| $\mathbf{J}$ | Electric current distribution |
| $j$ | $\sqrt{-1}$ |
| $k$ | Wavenumber at any frequency $f$ |
| $k_o$ | Wavenumber at frequency $f_o$ |
| $k_x$ | As defined in equation (8) |
| $k_y$ | As defined in equation (9) |
| $k_z$ | As defined in equation (10) |
| $I_i$ | Unknown current coefficients |
| MoM | Method of Moments |
| $M_n$ | $n$th moment of AWE ($n=0,1,2,3,4$ .....) |
| $n!$ | Factorial of number $n$ |
| PEC | Perfect Electric Conductor |
| $P(q, p)$ | Permutation Function |
| $R$ | Distance between the source point and the observation point |
| $\mathbf{r}_i$ | Coordinate of the node opposite to the edge $i$ |
| $\mathbf{r}$ | Coordinate of point in the triangle |
| $\mathbf{T}$ | Vector testing function as defined in equation (13) |

| | |
|---|---|
| $V(k)$ | Excitation vector as funtion of $k$ |
| $V^{(n)}(k_o)$ | $n$th derivative of $V(k)$ with respect to $k$; $\frac{d^n}{dk^n}V(k)$, evaluated at $k_o$ |
| **x** | Unit normal along X-axis |
| **y** | Unit normal along Y-axis |
| $Z(k)$ | Impedance matrix as a function of $k$ |
| $Z^{-1}(.)$ | Inverse of the matrix $Z(.)$ |
| $Z^{(q)}(k_o)$ | $q$th derivative of $Z(k)$ with respect to $k$; $\frac{d^q}{dk^q}Z(k)$, evaluated at $k_o$ |
| **z** | Unit normal along Z-axis |

# 1. Introduction

The Method of Moments (MoM) using the Electric Field Integral Equation (EFIE) has been a very useful tool for accurately predicting the Radar Cross Section (RCS) of arbitrarily shaped three dimensional PEC objects [1]. Implementation of MoM for EFIE involves solving for electric current using the vector and scalar potential solutions which satisfy the boundary condition that the tangential electric field at the boundary of the PEC body is zero. This is done by using Galerkin's technique and forming simultaneous equations. In a subdomain technique, the PEC body is divided into subdomains such as triangles, rectangles or quadrilaterals. The simultaneous equations are generated over the subdomains and added together to form a global matrix equation. This results in a dense, complex matrix, which can be solved either by a direct solver using LU decomposition or by an iterative solver using either conjugate gradient method or biconjugate gradient method. Generation of the matrix equation and its solution are the two major computationally intensive operations in MoM.

To obtain the frequency response of RCS using MoM, one has to repeat the calculations at every frequency over the frequency band of interest. If the RCS is highly frequency dependent, one needs to do the calculations at the finer increments of frequency to get an accurate representation of the frequency response. This can be computationally intensive and for electrically large objects it can be computationally prohibitive despite the increased power of the present generation of computers. To alleviate the above problems, the Asymptotic Waveform Evaluation (AWE) technique has been proposed. Applied to timing analysis of very large scale integrated (VLSI) circuits intially [2,3], it is finding increasing interest in electromagnetic analysis of microwave circuits [4,5]. Recently, a detailed description of AWE applied to

frequency domain electromagnetic analysis is presented in [6].

In this work, we describe the application of AWE for predicting RCS of the three dimensional PEC objects over a wide band of frequencies using the Method of Moments. In the AWE technique, the electric current is expanded in a Taylor series around a frequency. The coefficients of the Taylor series (called 'moments', not to be confused with moments in Method of Moments) are evaluated using the frequency derivatives of the EFIE. Once the moments are obtained, the electric current distribution on the PEC body can be obtained at any frequency within the bandwidth. Using this current distribution, the RCS is obtained.

The rest of the report is organized as described below. For the sake of completeness, in section 2, the MoM formulation of the EFIE is described briefly. In section 3, AWE implementation for the EFIE is described in detail. The frequency derivatives of EFIE are obtained and presented. Numerical results for a square plate, cube, and sphere are presented in section 4. The numerical data are compared with the exact solution over the bandwidth. CPU time and storage requirements for AWE formulation are given for each example and are compared with those required for exact solution at each frequency. Concluding remarks on the advantages and disadvantages of the AWE technique are presented in section 5.

# 2. MoM Implementation of EFIE

Consider an arbitrarily shaped PEC body shown in figure 1. For RCS calculations, a plane wave is assumed to be incident at an angle $(\theta_i, \phi_i)$ . At the surface of the PEC body, the total tangential electric field is zero. Writing the total tangential electric field in terms of the scattered

field and the incident field

$$\mathbf{E}_{scat} + \mathbf{E}_{inc} = 0 \tag{1}$$

The scattered electric field in terms of the equivalent electric current distribution on the PEC body is given by[7]

$$\mathbf{E}_{scat} = \frac{-jk\eta_o}{4\pi}\iint \mathbf{J}\frac{\exp(-jkR)}{R}ds' - \frac{jk}{4\pi\eta_o}\nabla\left(\iint(\nabla' \bullet \mathbf{J})\frac{\exp(-jkR)}{R}ds'\right) \tag{2}$$

and the incident electric field is given by

$$\mathbf{E}_{inc} = \mathbf{E}_i \exp[j(k_x x + k_y y + k_z z)] \tag{3}$$

where

$$\mathbf{E}_i = \mathbf{x}E_{xi} + \mathbf{y}E_{yi} + \mathbf{z}E_{zi} \tag{4}$$

and

$$E_{xi} = \cos\theta_i \cos\phi_i \cos\alpha - \sin\phi_i \sin\alpha \tag{5}$$

$$E_{yi} = \cos\theta_i \sin\phi_i \cos\alpha + \cos\phi_i \sin\alpha \tag{6}$$

$$E_{zi} = -\sin\theta_i \cos\alpha \tag{7}$$

$$k_x = k\sin\theta_i \cos\phi_i \tag{8}$$

$$k_y = k\sin\theta_i \sin\phi_i \tag{9}$$

$$k_z = k\cos\theta_i \tag{10}$$

$$R = \sqrt{(x-x')^2 + (y-y')^2 + (z-z')^2} \tag{11}$$

$k$ is the wavenumber corresponding to any frequency $f$. The source point is $(x', y', z')$ and

$(x, y, z)$ is the observation point. $\nabla'$ indicates the del operation with respect to the source coordinate system. $\alpha$ is the polarization angle [8]. The surface integral in equation (2) is evaluated over the surface of the PEC body.

In a subdomain MoM, the PEC surface is divided into subdomains such as triangles, rectangles and quadrilaterals. In this report we follow the triangular subdomain approach reported in [9]. The sample discretization of a square plate and a sphere with triangular subdomains are shown in figure 2. The electric current is expanded in rooftop basis functions over each triangle.

$$\mathbf{J} = \sum_{nt=1}^{3} I_{nt} \frac{l_{nt}}{2A} (\mathbf{r} - \mathbf{r}_{nt}) \tag{12}$$

A is the area of the triangle and the other parameters with respect to a triangle are shown in figure 3.

Equations (2) and (3) are substituted in equation (1), and following Galerkin's technique, equation (1) is mutiplied by a vector testing function $\mathbf{T}$ and integrated over the surface of a triangle [9].

$$\sum_{jt=1}^{N_e} \left[ \sum_{nt=1}^{3} I_{nt}^{(it)} \left\{ \frac{jk\eta_o}{4\pi} \iint_{it} \mathbf{T}_{mt}^{(it)} \bullet \iint_{jt} \mathbf{J}_{nt}^{(jt)} \frac{\exp(-jkR)}{R} ds' ds \right.\right.$$

$$\left.\left. - \frac{j\eta_o}{4\pi k} \iint_{it} \left( \nabla \bullet \mathbf{T}_{mt}^{(it)} \right) \iint_{jt} \left( \nabla' \bullet \mathbf{J}_{nt}^{(jt)} \right) \frac{\exp(-jkR)}{R} ds' ds \right\} \right]$$

$$= \iint_{it} \mathbf{T}_{mt}^{(it)} \bullet \mathbf{E}_{inc} ds \qquad mt=1,2,3;\ it=1,2,3, \ldots N_e \tag{13}$$

where

$$\mathbf{J}_{nt}^{(jt)} = \frac{l_{nt}^{(jt)}}{2A^{(jt)}}\left(\mathbf{r} - \mathbf{r}_{nt}^{(jt)}\right) \tag{14}$$

$$\mathbf{T}_{mt}^{(it)} = \frac{l_{mt}^{(it)}}{2A^{(it)}}\left(\mathbf{r} - \mathbf{r}_{mt}^{(it)}\right) \tag{15}$$

$N_e$ is the total number of triangles. Superscript *(jt)* is used to indicate the triangle containing the observation and superscript *(it)* is used to indicate the triangle containing the source point. The contributions from all the triangles over the surface are added to form a global matrix equation

$$Z(k)\, I(k) = V(k) \tag{16}$$

where

$$Z(k) = \sum_{jt=1}^{N_e}\left[\sum_{nt=1}^{3}\left\{\frac{jk\eta_o}{4\pi}\int\!\!\int_{it}\mathbf{T}_{mt}^{(it)} \bullet \int\!\!\int_{jt}\mathbf{J}_{nt}^{(jt)}\frac{\exp(-jkR)}{R}ds'ds\right.\right.$$

$$\left.\left. -\frac{j\eta_o}{4\pi k}\int\!\!\int_{it}\left(\nabla\bullet\mathbf{T}_{mt}^{(it)}\right)\int\!\!\int_{jt}\left(\nabla'\bullet\mathbf{J}_{nt}^{(jt)}\right)\frac{\exp(-jkR)}{R}ds'ds\right\}\right] \quad mt=1,2,3;\ \ it=1,2,3,\ldots.\ N_e \tag{17}$$

and

$$V(k) = \int\!\!\int_{it}\mathbf{T}_{mt}^{(it)} \bullet \mathbf{E}_{inc}ds \quad m=1,2,3;\ \ it=1,2,3,\ldots.\ N_e \tag{18}$$

In equation (17), $Z(k)$ is a complex, dense square matrix. $V(k)$ is the excitation vector and $I(k)$ is the vector with unknown current coefficients.

Equation (16) is solved at any specific frequency $f_o$ (with wavenumber $k_o$) either by a direct method using LU decomposition or by an iterative method using either conjugate gradient method or biconjugate gradient method. The advantage of direct method is that for multiple incident angles, the $Z(k_o)$ matrix has to be decomposed only once and for each incident angle the forward/backward substitutions are performed which are computationally less intensive.

The solution of equation (16) gives the unknown current coefficients $I(k_o)$ which are substituted in equation (12) to obtain the electric current distribution over all the triangles. Once the electric current distribution is known, the scattered electric far field is computed as [7]

$$\mathbf{E}_{fscat}(\mathbf{r})\Big|_{r\to\infty} = -jk_o\eta_o\frac{\exp(-jk_o r)}{4\pi r}\iint(\hat{\theta}\hat{\theta}+\hat{\phi}\hat{\phi})\bullet\mathbf{J}(x',y')\exp(jk_o\sin(\theta(x'\cos\phi+'y\sin\phi)+z'\cos\theta))\,dx'dy' \quad (19)$$

where $(r,\theta,\phi)$ are the spherical coordinates of the observation point. The radar cross section is given by

$$\sigma = \lim_{r\to\infty} 4\pi r^2\frac{\left|\mathbf{E}_{fscat}(\mathbf{r})\right|^2}{\left|\mathbf{E}_{inc}(\mathbf{r})\right|^2} \quad (20)$$

The radar cross section given in equation (20) is calculated for at one frequency. Given the proper sampling size of the discretization, this calculation is widely accepted in the RCS community as “exact” solution. If one needs RCS frequency response, this calculation is to be repeated at different frequency values.

# 3. AWE Implementation

The general implementation of AWE for any frequency domain technique used for electromagnetic analysis is given in detail in [6]. As shown in the previous section, the solution of equation (16) gives the unknown current coefficient vector $I(k_o)$ at a particular frequency $f_o$. Instead $I(k)$ can be expanded in Taylor series as

$$I(k) = \sum_{n=0}^{\infty} M_n (k - k_o)^n \tag{21}$$

with the moments $M_n$ given by [6]

$$M_n = Z^{-1}(k_o) \left[ \frac{V^{(n)}(k_o)}{n!} - \sum_{q=0}^{n} \frac{(1 - \delta_{qo}) Z^{(q)}(k_o) M_{n-q}}{q!} \right] \tag{22}$$

$Z^{(q)}(k_o)$ is the *q*th derivative with respect to *k* of *Z(k)* given in equation (17) and evaluated at $k_o$. Similarly, $V^{(n)}(k_o)$ is the *n*th derivative with respect to *k*, of *V(k)* given in equation (18) and evaluated at $k_o$. The Kronecker delta $\delta_{qo}$ is defined as

$$\delta_{qo} = \begin{cases} 1 & q = 0 \\ 0 & q \neq 0 \end{cases} \tag{23}$$

The evaluation of $Z^{(q)}(k)$ is a lengthy process, due to the presence of $1/k$ in the second term of equation (17). The derivatives can be obtained by successively diffrentiating the previous derivative of $Z(k)$. Alternatively each deriavtive can be independently obtained by using the product rule [10]:

$$\frac{d^q}{dk^q}[uv] = \binom{q}{0} v\frac{\partial^q u}{\partial k^q} + \binom{q}{1}\frac{\partial v}{\partial k}\frac{\partial^{q-1} u}{\partial k^{q-1}} + \binom{q}{2}\frac{\partial^2 v}{\partial k^2}\frac{\partial^{q-2} u}{\partial k^{q-2}} + \text{.....} +$$

$$\binom{q}{p}\frac{\partial^p v}{\partial k^p}\frac{\partial^{q-p} u}{\partial k^{q-p}} + \text{.....} + \binom{q}{q} u\frac{\partial^q v}{\partial k^q} \qquad (24)$$

where $\binom{q}{p} = \frac{q!}{p!\,(q-p)!}$ the binomial coefficient, q non-negetive integer and $\binom{q}{0} = 1$.

On the right hand side of equation (17), the derivatives of the two terms can be obtained by setting

$$u = \frac{jk\eta_o}{4\pi}$$

and

$$v = \int\int_{it} \mathbf{T}_{mt}^{(it)} \bullet \int\int_{jt} \mathbf{J}_{nt}^{(jt)} \frac{\exp(-jkR)}{R} ds'ds$$

in the first term and

$$u = -\frac{j\eta_o k^{-1}}{4\pi}$$

and

$$v = \int\int_{it}\left(\nabla\bullet\mathbf{T}_{mt}^{(it)}\right)\int\int_{jt}\left(\nabla'\bullet\mathbf{J}_{nt}^{(jt)}\right)\frac{\exp(-jkR)}{R} ds'ds$$

in the second term. The derivatives of the two terms can be obtained independently and added together to get $Z^{(q)}(k)$. After performing a number of differentiations, it can be shown that the explicit and compact representation of $Z^{(q)}(k_o)$ is given by [6]

$$Z^{(q)}(k_o) = \sum_{jt=1}^{N_e}\left[\sum_{nt=1}^{3}\left\{\frac{jk\eta_o}{4\pi}\int\!\!\int_{it}\mathbf{T}_{mt}^{(it)}\bullet\int\!\!\int_{jt}\mathbf{J}_{nt}^{(jt)}(-jR)^q\left(1-\frac{q}{jk_oR}\right)\frac{\exp(-jkR)}{R}ds'ds\right.\right.$$

$$\left.\left.-\frac{j\eta_o}{4\pi k}\int\!\!\int_{it}\left(\nabla\bullet\mathbf{T}_{mt}^{(it)}\right)\int\!\!\int_{jt}\left(\nabla'\bullet\mathbf{J}_{nt}^{(jt)}\right)(-jR)^q\left(\sum_{p=0}^{q}\frac{P(q,p)}{(jk_oR)^p}\right)\frac{\exp(-jkR)}{R}ds'ds\right\}\right]$$

$$mt=1,2,3;\ \ it=1,2,3,\ldots.\ N_e \qquad (25)$$

where the permutation function *P(q,p)* is defined as [11]

$$P(q,p) = \frac{q!}{(q-p)!} \qquad (26)$$

The expression for $V^{(n)}(k_o)$ is given by

$$V^{(n)}(k_o) = (j)^n\int\!\!\int\mathbf{T}_{mt}^{(it)}\bullet\mathbf{E}_i(X_1+Y_1+Z_1)^n\exp(jk_o(X_1+Y_1+Z_1))\,ds$$

$$mt=1,2,3;\ \ it=1,2,3,\ldots.\ N_e \qquad (27)$$

where $X_1 = x\sin\theta_i\cos\phi_i$, $Y_1 = y\sin\theta_i\sin\phi_i$ and $Z_1 = z\cos\theta_i$.

Substituting equations (25) and (27) in equation (22), the moments of AWE are obtained. Using these moments, the current coefficients at frequencies around the expansion frequency are obtained by using equation (21). The electric current distribution over each triangular subdomain is obtained using equation (12). Using equations (19) and (20), the radar cross section at frequencies around the expansion frequency can be calculated.

# 4. Numerical Results

To validate the analysis presented in the previous sections, a few numerical examples are considered. RCS frequency response calculations are done for a square plate, a cube, and a

sphere. The numerical data obtained using AWE are compared with the results calculated at each frequency using the triangular patch Method of Moments. We will refer to the later method as "exact solution." All the computations reported below are done on a CONVEX C-220 computer.

## (a) Square Plate:

First example is a square plate ($1cm \times 1cm$, figure 4(a)) with the incident electric field at $\theta_i = 90^o$ and $\phi_i = 0^o$. The incident field is E-polarized ($\alpha = 90^o$). The RCS frequency response is calculated with 12 GHz as the expansion frequency. The AWE moments are calculated at 12 GHz and are used in the Taylor series expansion. The frequency response from 9 GHz to 15 GHz is plotted in Figure 4(b) along with the exact solution calculated at different frequencies. A very good agreement can be seen between the AWE frequency response and the exact solution over the bandwidth. The frequency response is calculated using 8th order AWE. The frequency response calculation using 5th order AWE is also plotted in figure 4. For 307 unknowns, exact solution took around 262 seconds CPU time to fill the matrix and 1.6 seconds CPU time to LU factor the matrix at each frequency. AWE frequency response calculation took 1187 seconds CPU time to fill the matrices including the frequency derivative matrices and 1.6 seconds CPU time to LU factor the matrix. The exact solution was carried out at 7 frequencies, whereas, with AWE the frequency response is calculated at frequency increments of 0.1 GHz. There is a substantial amount of savings in CPU time by using AWE, when RCS frequency response is required with fine frequency increments.

Another example of RCS frequency response of the square plate is considered in the frequency range 25 GHz to 35 GHz. The square plate is discretized with 603 unknowns. The

AWE frequency response is calculated using 8th order Taylor series expansion. The RCS frequency response with a E-polarized ($\alpha = 90^o$) incident wave at $\theta_i = 90^o$ and $\phi_i = 0^o$ is plotted from 25 GHz to 35 GHz in figure 5. The frequency response calculation using 6th order AWE is also plotted in figure 5. All the moments of AWE are calculated at 30 GHz. It can be seen from figure 5 that AWE frequency response agrees well with the eaxct solution at each frequency. AWE frequency response is calculated at 0.1 GHz increments. AWE took 4470 seconds CPU time to fill the matrices, including the derivative matrices, whereas exact solution took 909 seconds for matrix fill at each frequency (i.e., 9090 seconds for 10 frequencies). The LU factorization took 12.4 seconds CPU time for AWE, whereas it took 12.5 seconds CPU time for exact solution at each frequency calculation (125 seconds for 10 frequencies).

## (b) Cube

RCS frequency response of a cube ($1cm \times 1cm \times 1cm$, fig. 6(a)) is computed using AWE for normal incidence. The frequency response is calculated with 11 GHz as the expansion frequency and plotted in figure 6(b) over the frequency band 8 GHz to 14 GHz. The results are plotted both for 4th order AWE and 8th order AWE. AWE frequency response is calculated with 0.1 GHz frequency increment. The cube is discretized with 348 triangular patches resulting in 522 unknowns. A good agreement between the AWE results and the exact solution can be seen. Even the 4th order AWE gave accurate results except in the end of the band region. The 4th order AWE took 1512 seconds CPU time for filling the matrices including the derivative matrices and 8 seconds CPU time for LU factorization. The 8th order AWE took 3082 seconds CPU time for filling up the matrices including the derivative matrices and 8 seconds CPU time for LU factorization. The exact solution took about 613 seconds CPU time to fill the matrix

(4291 seconds for 7 frequencies) and 8 seconds CPU time for LU factorization (56 seconds for 7 frequencies).

## (c) Sphere

As a third example, a PEC sphere of radius 0.318cm is considered. To demonstrate the usefulness of AWE over a wide bandwidth, three frequency points are considered at 20 GHz, 30 GHz and 40 GHz to obtain RCS frequency response over the frequency range 15 GHz to 45 GHz. The sphere is discretized into 248 triangular elements at 20 GHz and 30 GHz and 504 triangular elements at 40 GHz. The frequency response is plotted in figure 7 along with the exact solution calculated with 1 GHz frequency interval over the bandwidth. It can be seen that AWE frequency response agrees well with the exact solution. It can be noted that even the 4th order AWE is sufficient to obtain the accurate frequency response over the bandwidth. The CPU timings for matrix fill and LU factorizations are given in Table 1. It can be seen from Table 1 that the exact solution with a frequency interval of 1 GHz took around 6hours of CPU time to calculate the frequency response over the frequency bandwidth (15 GHz to 45 GHz), AWE calculation requires only 1 hour and 22 minutes of CPU time.

**Table 1: CPU timings for RCS frequency response calculation of a PEC sphere**

| Method | Frequency Band (GHz) | | | | | |
|---|---|---|---|---|---|---|
| | 15GHz-25GHz (372 unknowns) | | 25GHz-35GHz (372unknowns) | | 35GHz-45GHz (756 unknowns) | |
| | Matrix Fill (secs) | LU Factor (secs) | Matrix Fill (secs) | LU Factor (secs) | Matrix Fill (secs) | LU Factor (secs) |
| AWE_MoM (4th order) | 828 | 3 | 828 | 3 | 3211 | 25 |

**Table 1: CPU timings for RCS frequency response calculation of a PEC sphere**

| Method | Frequency Band (GHz) | | | | | |
|---|---|---|---|---|---|---|
| | 15GHz-25GHz (372 unknowns) | | 25GHz-35GHz (372unknowns) | | 35GHz-45GHz (756 unknowns) | |
| | Matrix Fill (secs) | LU Factor (secs) | Matrix Fill (secs) | LU Factor (secs) | Matrix Fill (secs) | LU Factor (secs) |
| MoM (10 Frequency Points) | 3710 | 30 | 3710 | 29 | 14,220 | 250 |

***Comment on Storage***: In all the above examples, when solving a matrix equation, one needs to store a complex, dense matrix $Z(k_o)$ of size $\mathrm{N} \times \mathrm{N}$ for exact solution at each frequency. For $n^{\text{th}}$ order AWE, one needs to store *n* number of complex, dense matrixes ($Z^{(q)}(k_o)$ , *q=1,2,3,...n*) of size $\mathrm{N} \times \mathrm{N}$, along with the matrix $Z(k_o)$ of size $\mathrm{N} \times \mathrm{N}$. For electrically large problems, this could impose a burden on computer resources. This problem can be overcome by storing the derivative matrices, $Z^{(q)}(k_o)$ out-of-core, as the derivative matrices are required only for matrix-vector multiplication.

# 5.0 Concluding Remarks

An implementation of AWE for frequency domain Method of Moments is presented. The RCS frequency response for different PEC objects such as a square plate, cube, and sphere are computed and compared with the exact solution. It is also found to be useful to use multi-frequency expansion points to get wide frequency bandwidth. From the numerical examples presented in this report, AWE is found to be superior in terms of the CPU time to obtain a frequency response. It may also be noted that although calculations are done at one incidence

angle  for all the examples presented, with a nominal cost, the frequency response at multiple incidence angles can also be calculated. AWE is accurate at and around the frequency of expansion and the accuracy deteriorates beyond certain bandwidth. The accuracy of AWE over a desired frequency band and its relation to the order of AWE to be used are topics of interest for future research. With these topics addressed, AWE will be of good use in computing the frequency response using a frequency domain technique such as Method of Moments.

# References


[1] E.K.Miller, L. Medgysi-Mitschang and E.H.Newman(Eds), *Computational Electromagnetics: Frequency domain method of moments*, IEEE Press, New York, 1992.

[2] L.T.Pillage and R.A.Rohrer, "Asymptotic waveform evaluation for timing analysis," *IEEE Trans. Computer Aided Design*, pp. 352-366, 1990.

[3] T.K.Tang, M.S.Nakhla and R.Griffith, "Analysis of lossy multiconductor transmission lines using the asymptotic waveform evaluation technique," *IEEE Trans. Microwave Theory and Techniques*, Vol.39, pp.2107-2116, December 1991.

[4] D.Sun, J.Manges, X.Yuan and Z.Cendes, "Spurious modes in finite element method," *IEEE Antennas and Propagation Magazine*, Vol.37, pp.12-24, October 1995.

[5] J. Gong and J.L.Volakis, "An AWE implementation of electromagnetic FEM analysis," *personal communication.*

[6] C.R.Cockrell and F.B.Beck, "Asymptotic Waveform Evaluation (AWE) technique for frequency domain electromagnetic analysis," *NASA Technical Memorandum 110292*, 1996.

[7] R.F.Harrington, *Time-Harmonic Electromagnetic Fields*, McGraw-Hill Book Co., Inc. 1961.

[8] C.A.Balanis, *Advanced Engineering Electromagnetics*, John Wiley & Sons, New York, 1989.

[9] S.M.Rao, "Electromagnetic scattering and radiation of arbitrarily shaped surfaces by triangular patch modelling," *Ph.D. Thesis*, The University of Mississippi, August 1980.

[10] W.H.Beyer(Ed.), *CRC Standard mathematical tables*, 27th Edition, pp.228, CRC Press Inc., Boca Raton FL, 1984.

[11] M.Fogiel, *Handbook of Mathematical, Scientific and Engineering Formulas, Tables, Functions, Graphs, Transforms*, Research and Education Association, New York NY, 1985, pp.85.

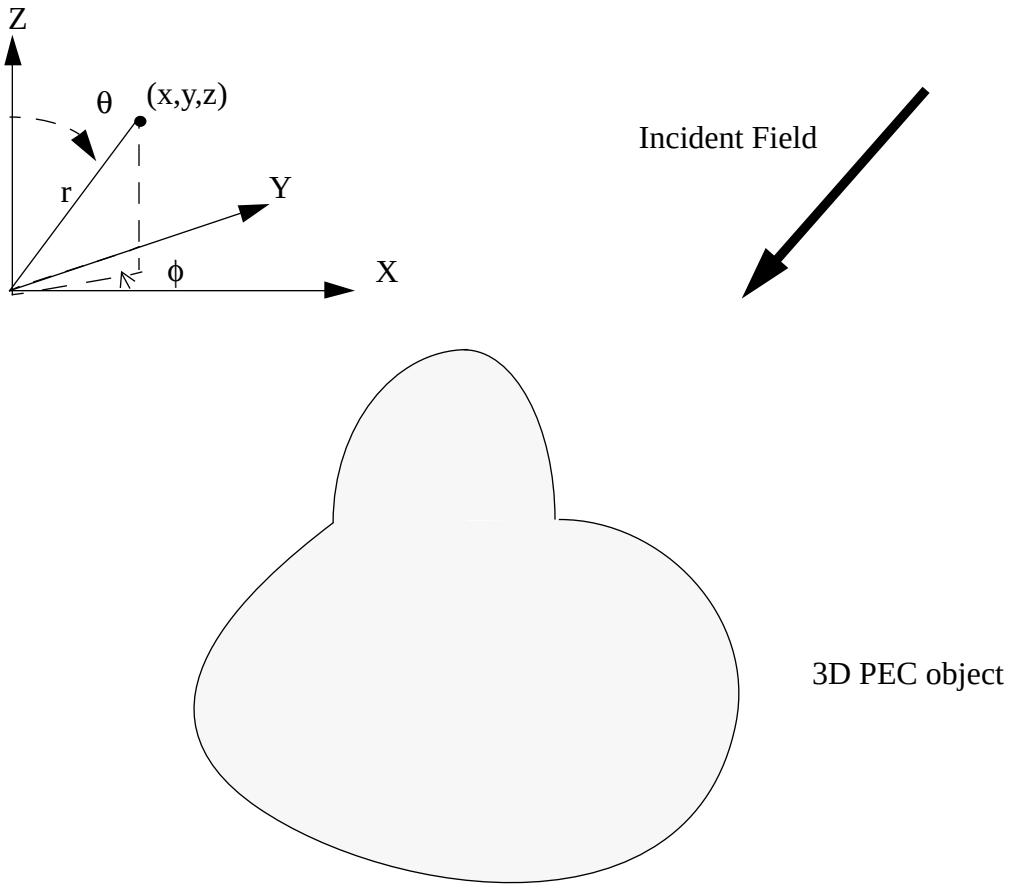


Figure 1 Arbitrarily shaped three dimensional PEC object

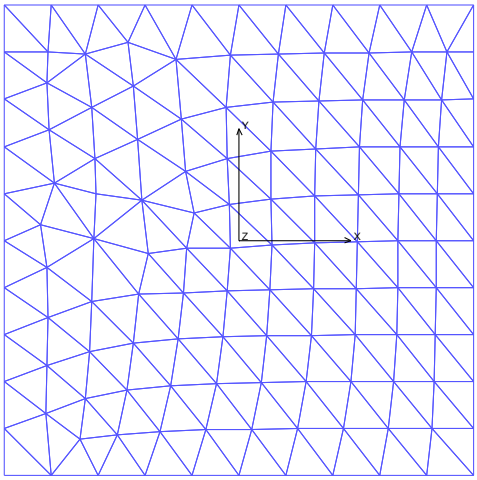


(a)

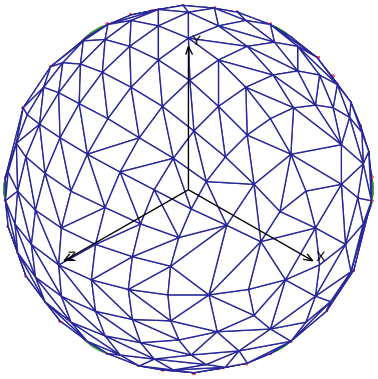


(b)

Figure 2 Triangular discretization of the three diemnsional PEC objects. (a) Square plate - As the normal component of the electric current is zero on the edges, the current coefficients are set to zero on the edges (b) Sphere.

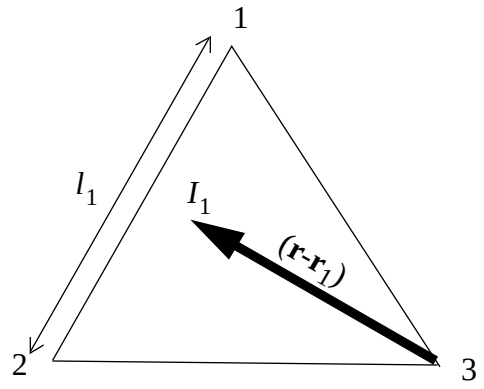


(a) Edge 1

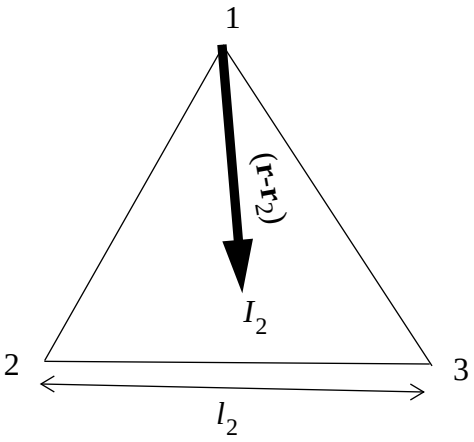


(b) Edge 2

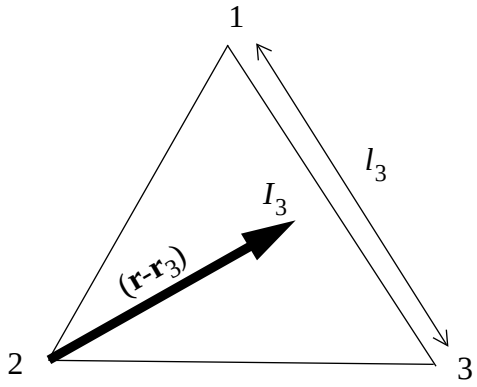


(c) Edge 3

Figure 3 The current basis function as defined in equation (7) for the three edges of the triangle.

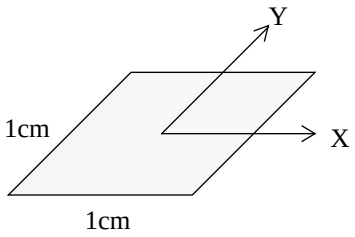


(a)

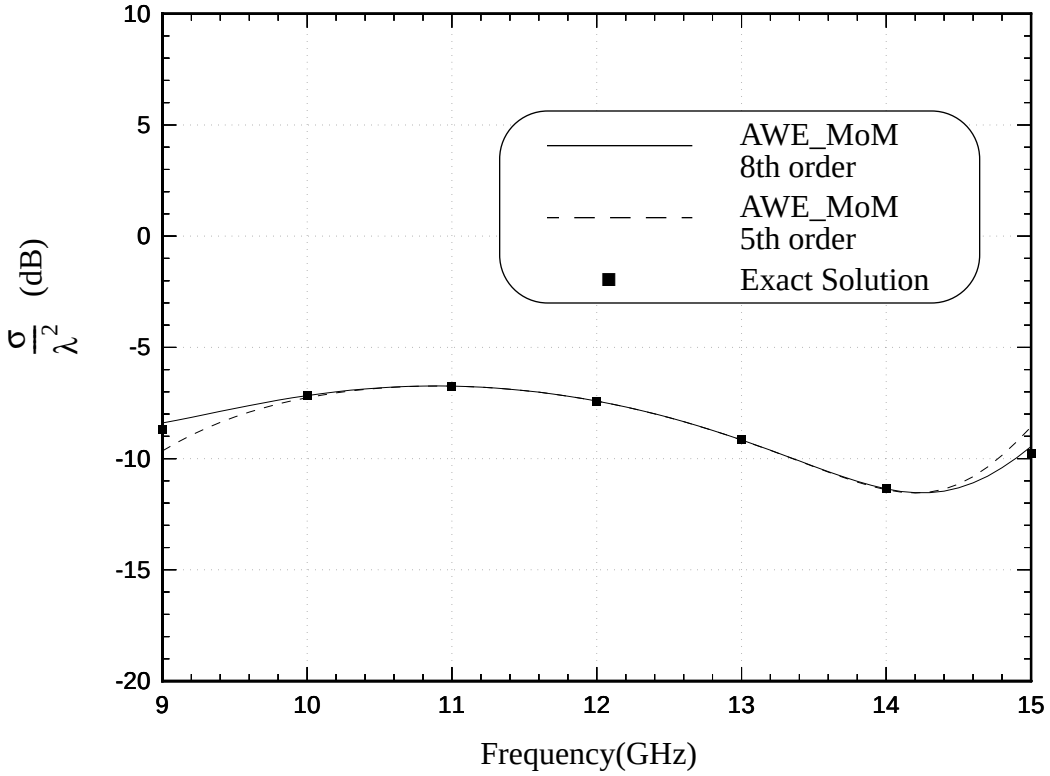


(b)

Figure 4(a) Square Plate (1cmX1cm)
(b) RCS frequency response the square plate(1cmX1cm) from 9GHz to 15GHz

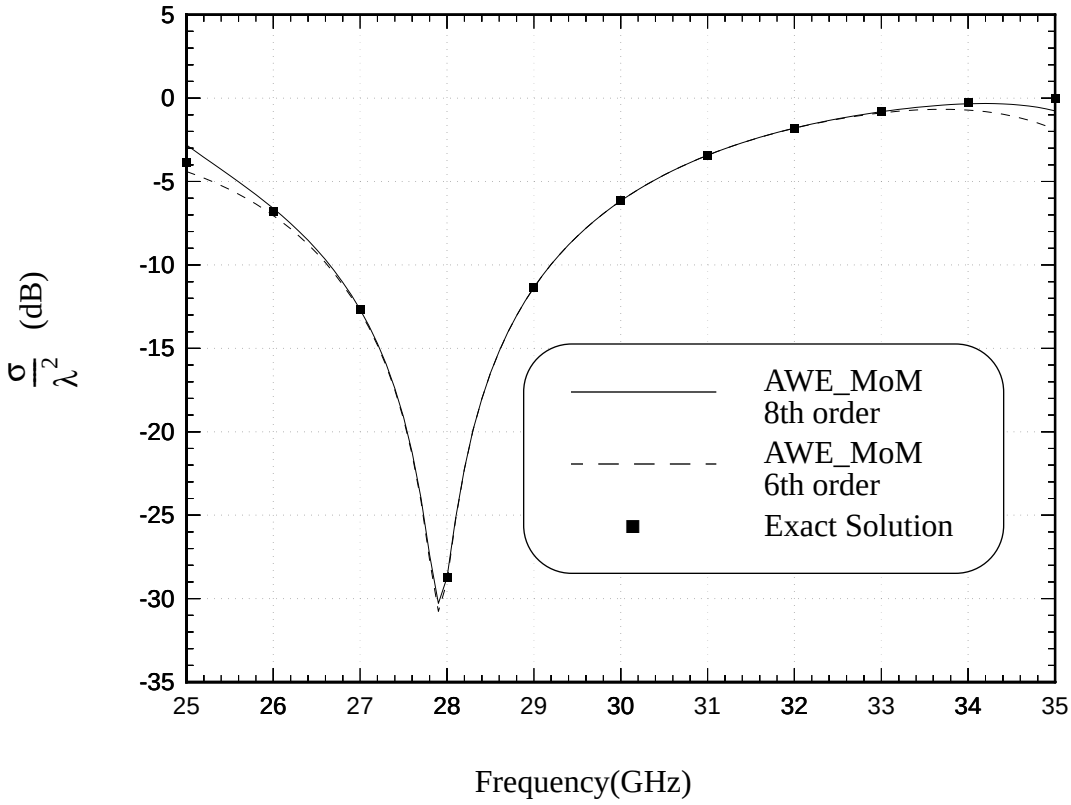


Figure 5 RCS frequency response of the square plate(figure 4(a)) from 25GHz to 35GHz

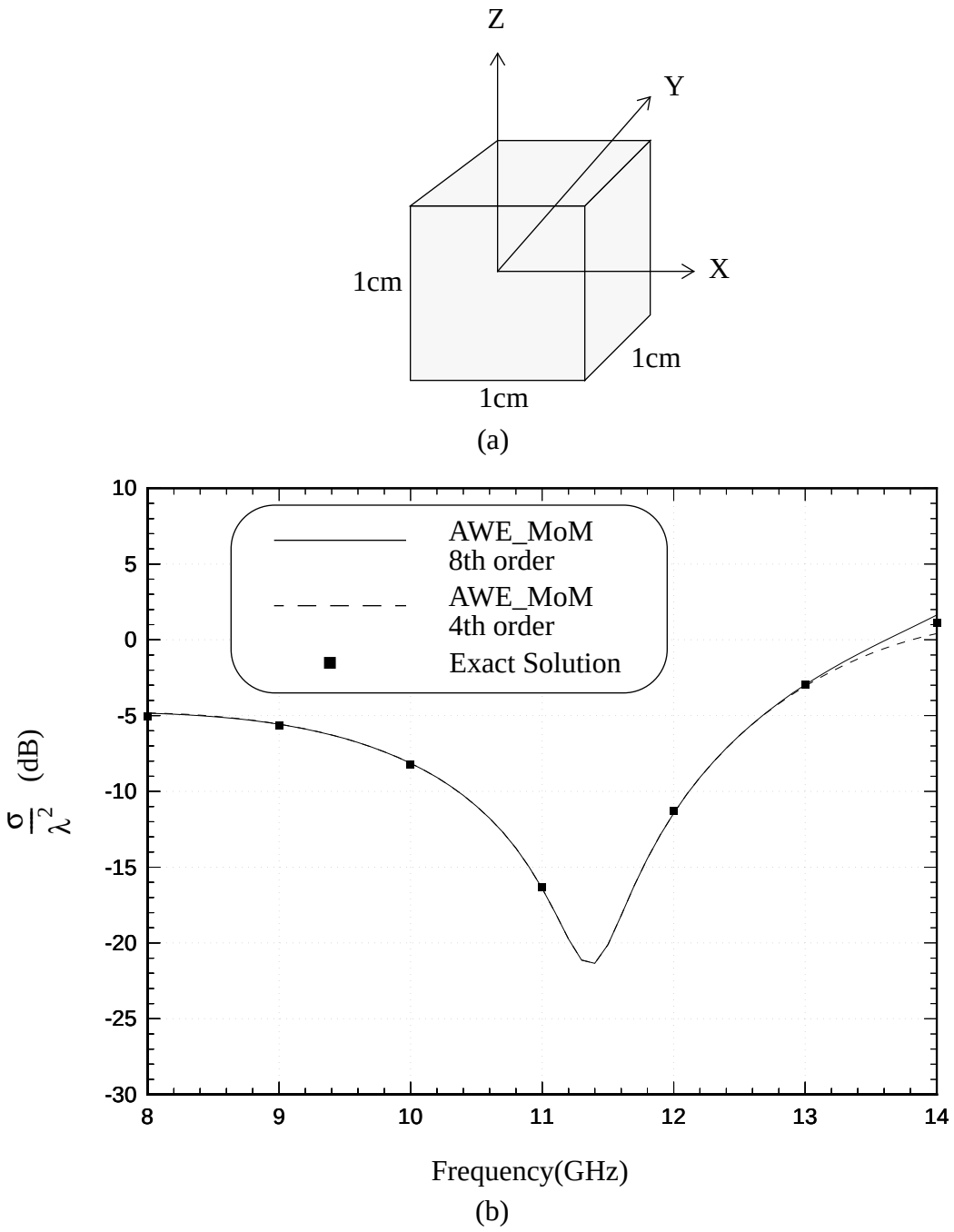


Figure 6(a) A PEC cube (1cmX1cmX1cm)
(b) RCS frequency response of the cube from 9GHz to 15GHz

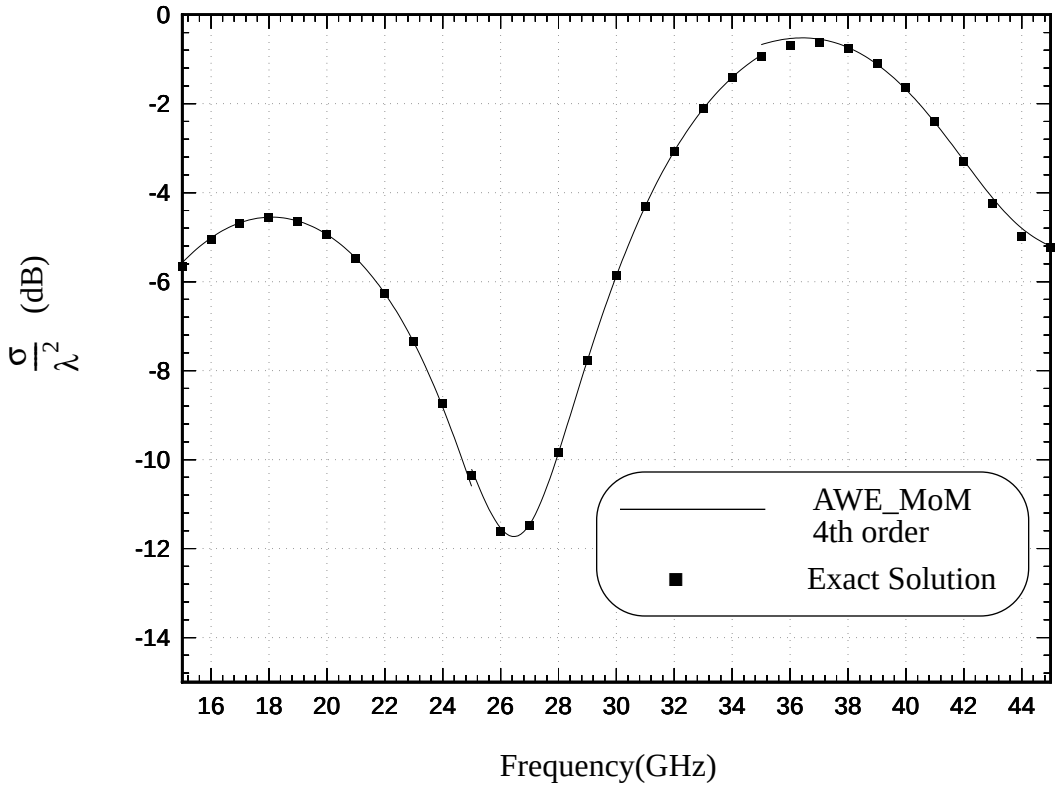


Figure 7 RCS frequency response of a sphere (radius=0.318cm) from 15GHz to 45GHz using three frequency expansion points at 20GHz, 30GHz and 40GHz